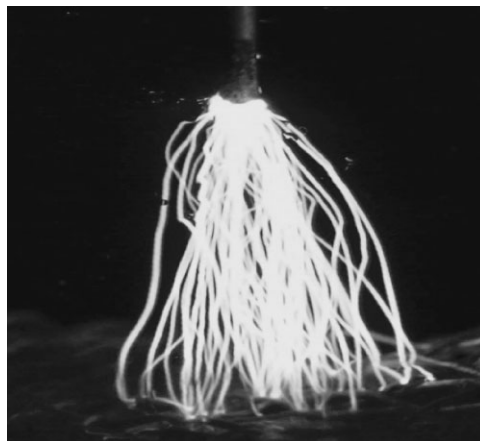


Formation of ROS and RNS in Water Electro-Sprayed through Transient Spark Discharge in Air and their Bactericidal Effects

Zdenko Machala,* Barbora Tarabova, Karol Hensel, Eva Spetlikova, Libusa Sikurova, Petr Lukes

Chemical and bactericidal effects induced by plasma in water upon electro-spraying through DC-driven positive transient spark discharge in air were investigated. Inactivation of *E. coli* was determined in dependence on pH (controlled by buffers) and correlated with chemical changes induced in water. Productions of hydrogen peroxide, nitrites, nitrates, peroxyxynitrites, and pH changes were determined, and the extent of oxidative stress induced in bacteria was evaluated. The degree of inactivation and oxidative damage of bacteria increased with the increasing acidity of the solution. Acidified nitrites interacting with hydrogen peroxide were determined as the most important bactericidal ROS/RNS agents in plasma-treated water. A possible role of peroxyxynitrites, ozone, and metal nanoparticles is discussed.



1. Introduction

A great number of recent publications on plasma decontamination and plasma medicine witness a quick evolution and a great potential of this new interdisciplinary field. Nowadays it is evident that cold atmospheric pressure plasmas can efficiently kill various microbes, even highly resistant forms such as bacterial spores and biofilms,

and foster interesting phenomena in the cells of higher organisms leading to various therapeutic effects. The mechanisms of plasma–cell interaction are not fully understood yet, although a great research effort has been dedicated to elucidate the respective roles of various plasma agents in the interaction with live cells, such as charged particles, neutral reactive species, UV radiation, electric field, and heat.^[1] Most studies agree on that the bactericidal effects of atmospheric pressure cold plasmas are dominantly due to reactive neutral species (mainly radicals) and perhaps some ions (such as superoxide anion O₂⁻).

For many practical applications, bio-decontamination under wet conditions is important. In parallel, plasma medical applications deal with cells and tissues in their naturally humid environment. When cells (e.g., bacteria) are immersed in a liquid or in a gel-like material with water content, neither ions nor electrons can interact directly with the cells as they are strongly absorbed by the liquid when applied through the gas–liquid interface. In these processes, plasmas induce various chemical effects leading

Z. Machala, B. Tarabova, K. Hensel, L. Sikurova
Faculty of Mathematics, Physics and Informatics, Comenius
University, Mlynská dolina, 84248 Bratislava, Slovakia
E-mail: machala@fmph.uniba.sk
E. Spetlikova
Institute of Plasma Physics AS CR, Za Slovankou 3, Prague 8,
18200, Czech Republic
Institute of Chemical Technology, Technicka 5, Prague 6, 16628,
Czech Republic
P. Lukes
Institute of Plasma Physics AS CR, Za Slovankou 3, Prague 8,
18200, Czech Republic

to active species that can interact with cells in the liquid environment, either leading to bactericidal effect, or various complex processes in eukaryotic cells resulting in therapeutic effects, or both.^[2] So it is very important to investigate the chemical effects of plasma in water directly cross-linked with the effects induced in cells.

Plasmas generated in air and in contact with water are of the great interest in the plasma decontamination and plasma medicine community because they produce large quantities of reactive oxygen species (ROS) and reactive nitrogen species (RNS) that seem to be the most efficient biocidal agents in bio-decontamination by plasma.^[3–9] Biological and therapeutic effects of air spark-like discharges on tissues have been demonstrated.^[10–12] Even rare gas plasma jets perform the strongest bactericidal efficacy with O₂ or air admixtures.^[2] Air plasma treatment of water and aqueous solutions typically leads to acidification,^[2,3,13–18] which can normally be explained by dissolution of NO_x species formed by air plasma in water.^[2,13–16] Acid environment itself, despite being crucial for the bactericidal effect in plasma treated water, did not prove to be the main antibacterial agent. Several authors reported that addition of various acids resulting in the same pH as in the plasma treated solutions (usually pH 2.5–4.8) did not lead to the same bactericidal efficacy. It was shown that the synergy of acid environment with plasma agents lead to the strong bacterial inactivation.^[2,13,14] However, it is not clear enough yet, which plasma agents and which ROS/RNS have dominant roles in water bio-decontamination and plasma medical applications, and what is the associated plasma-induced water chemistry. Hydrogen peroxide, nitrate, and nitrite anions, as well as other species such as peroxyxynitrites, have been identified or predicted in plasma-activated water but the complete image of chemical processes and their link to the associated bactericidal effects remains unclear.^[2,3,7,8,13,14,19]

The principal objective of this work is fundamental understanding of water chemistry during and following air plasma treatment and its direct link to the viability of bacterial cells. The treated water was electro-sprayed through a DC-driven positive transient spark discharge to enhance its interaction with the plasma. We measured pH, conductivity, and the concentrations of hydrogen peroxide (H₂O₂), nitrites (NO₂⁻), nitrates (NO₃⁻), and peroxyxynitrites (ONOO⁻) in the plasma treated water. Production of these chemical species was correlated with the pH changes and with bactericidal effects observed on *Escherichia coli* suspended in plasma treated solutions, and with the oxidative stress induced in cell membranes of these bacteria. We also treated buffered solutions and compared the chemical and bactericidal effects to their non-buffered counterparts to better understand the chemistry in relation to pH. This work follows our previous

studies of bio-decontamination of electro-sprayed water in the transient spark.^[20,21]

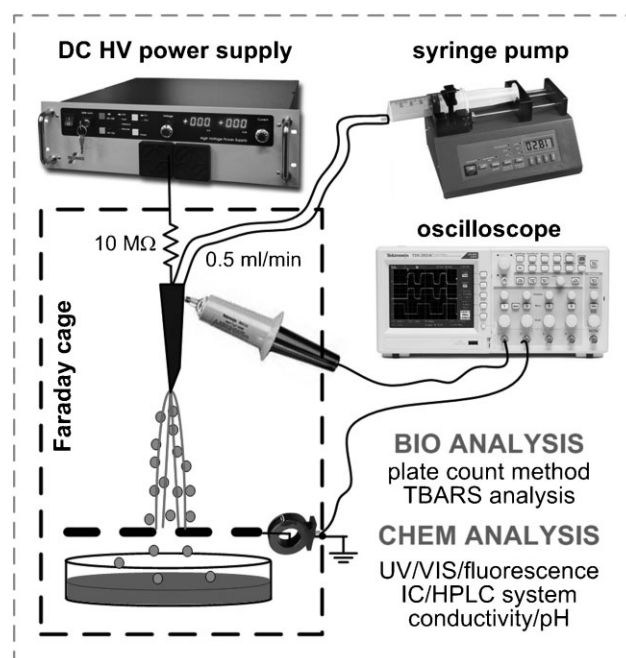
2. Experimental Section

2.1. Discharge Set-Up and Electrical Measurements

The experimental setup for DC-driven transient spark discharge in point-to-plane geometry is depicted in Figure 1. A high voltage (HV) hypodermic hollow needle electrode enabled us to inject aqueous solutions through the discharge zone with a constant flow rate 0.5 mL · min⁻¹. The inter-electrode spacing from the HV needle to the grounded mesh electrode was usually kept at 10 mm. A positive DC HV was applied through the ballast resistor *R* (10 MΩ). The discharge voltage was measured by a HV probe *Tektronix P6015A*. The discharge current was measured on a 1 Ω resistor or by a Rogowski current monitor *Pearson Electronics 2877*. The current and voltage signals were processed by a digitizing 200 MHz oscilloscope *Tektronix TDS 2024*. The discharges were photo-documented with a digital camera *Olympus E410*. The effect of electrostatic spraying of treated aqueous solutions injected directly through the HV needle electrode occurred when the HV was applied to the needle.^[20–22] The typical discharge visual appearance is shown in the photograph in Figure 2.

2.2. Treated Microorganisms, Microbial Handling, and Cultivation Procedure

Bactericidal effects were tested on Gram-negative bacteria *Escherichia coli* (CCM3954) suspended in water in planktonic form with initial populations from 10⁷ to 10⁸ colony forming units



■ Figure 1. The experimental setup with electro-spray of water.

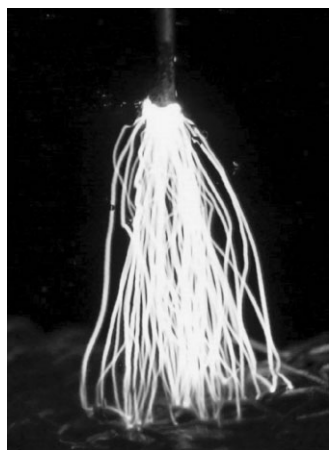


Figure 2. Photograph of the transient spark with electro-spray of water in 10 mm gap, water flow rate $0.5 \text{ mL} \cdot \text{min}^{-1}$, 14 kV.

per mL (CFU mL^{-1}). The microbial cultivation was carried out in a sterile environment in the following steps: an overnight bacterial culture was prepared in a shaker with sterile liquid nutrient. Bacteria cultivated in the liquid nutrient were compared with McFarland turbidity scale to assess their initial population per mL. They were then centrifuged several times and diluted in water/saline solutions to obtain desired concentrations. Alternatively, bacteria pre-cultivated on gel disks were directly dissolved in the desired solutions under study.

The plasma experiments with bacteria suspensions were performed with positive transient spark and repeated 10–15 times. The number of bacteria cells in the suspension was evaluated immediately after plasma treatment by counting colony forming units (CFUs) cultivated on agar plates (*MFC*, *HiMedia*, *Mumbai, India*; *Biolab*) during 12–24 h at 37°C . Several 10-fold dilution series were used to achieve optimum number of CFUs grown on agar plates (30–300), especially for controls and low inactivation rates. For high inactivation rates of plasma treated water or saline solution (≈ 6 logs reduction), no dilutions were needed. The dilution procedure was optimized empirically in several first sets of experiments. The lower detection limit of $2 \text{ CFU} \cdot \text{mL}^{-1}$ was calculated from the case when no dilution was applied (plasma treated water) and 0.5 mL of the treated sample was spread on the agar plate giving rise to at least one colony.

Usually, 3–4 agar plates from each sample were taken for statistical evaluation. The viability of bacteria was determined as the ratio of the population of surviving bacteria in plasma treated samples to the total population in reference samples.

In some experiments, the bacteria suspensions after plasma treatment were stored for 5 h in closed glass containers under room temperature for further analysis and comparison with fresh samples taken immediately post plasma treatment, and then cultivated on agar plates.

2.3. Measurements of the Oxidative Stress

One of the possible interactions of ROS with bacterial cell membranes is the peroxidation of membrane lipids. The

final product of lipid peroxidation is malondialdehyde (MDA), quantifiable by colorimetric method by the reaction with thiobarbituric acid (TBA) at $90\text{--}100^\circ\text{C}$. This widely used method of *thiobarbituric acid reactive substances* (TBARS) was applied to measure the oxidative stress induced in bacteria in water exposed to the discharge, similar to ref.^[9] The TBARS concentrations were determined from the absorbance of MDA measured at 532 nm by using molar absorption coefficient $\epsilon = 1.57 \times 10^5 \text{ L} \cdot \text{mol}^{-1} \cdot \text{cm}^{-1}$.^[21]

2.4. Measurements of Chemical Changes in Plasma Treated Water

Measurements of *hydrogen peroxide* formed in plasma treated water were performed by titanium sulfate colorimetric method using UV/VIS spectrophotometer *Unicam Helios Gamma* and UV/VIS/Fluorescence microplate reader *Thermo Scientific Varioskan Flash*. The titanium sulfate method for H_2O_2 was described by Eisenberg.^[23] The intense yellow color is formed when an acidic solution of titanyl ions are mixed with H_2O_2 . The method is specific to H_2O_2 and there are no interferences from other compounds present in water, while working under strong acidic conditions following the modified procedure of Satterfield and Bonnel.^[24] The formed yellow-colored complex of pertitanic acid H_2TiO_4 is stable for at least 6 h.^[23] The Lambert-Beer's law is followed and the yellow color intensity is proportional to the H_2O_2 concentration giving a linear relationship. The molar extinction coefficient determined in our laboratory from the slope of the calibration plot at the wavelength 407 nm was $\epsilon = 6.89 \times 10^2 \text{ L} \cdot \text{mol}^{-1} \cdot \text{cm}^{-1}$. The method is independent of the pH since the measurement of H_2O_2 is carried out in strong acidic solution of sulfuric acid (dilute 1:1). In the presence of nitrites, solution of sodium azide was added to the samples with H_2O_2 prior to mixing with titanium reagent to eliminate decomposition of H_2O_2 by nitrites under acidic conditions. With sodium azide, nitrites are reduced into molecular nitrogen under acidic conditions.^[25]

The concentrations of nitrites and nitrates were measured by ion chromatography using a HPLC system *Shimadzu LC-10Avp* with UV (210 nm) and suppressed conductivity detection. Analyses were made by means of a $7\text{-}\mu\text{m}$ *Allsep A1* anion exchange column ($10 \text{ cm} \times 4.6 \text{ mm}$) with $0.85 \text{ mmol} \cdot \text{L}^{-1} \text{ NaHCO}_3/0.9 \text{ mmol} \cdot \text{L}^{-1} \text{ Na}_2\text{CO}_3$ as the eluent (flow rate of $1.2 \text{ mL} \cdot \text{min}^{-1}$). Samples for ion chromatography analysis were fixed by phosphate buffer ($2 \text{ mmol} \cdot \text{L}^{-1} \text{ Na}_2\text{HPO}_4/\text{KH}_2\text{PO}_4$ solution, pH 6.9) immediately after being withdrawn from the plasma treated solution to stop acidic decomposition of nitrites, and then injected into chromatography column within 3 min after withdrawal.

Peroxynitrite concentration was determined by the reaction with 2,7-dichlorodihydrofluorescein diacetate (DCFH-DA) that converts to its highly fluorescent form dichlorofluorescein (DCF) under the action of ROS. Absorbance measurements at 500 nm and fluorescence measurements using excitation and emission wavelengths of 502 and 523 nm, respectively, were done according to the recommended procedure of the DCFH-DA assay fluorescence kit.^[26,27] The peroxynitrite fluorescence spectroscopy measurement was performed on *PerkinElmer LS 45*. Samples withdrawn from the plasma treated solutions were immediately fixed by a phosphate buffer ($2 \text{ mmol} \cdot \text{L}^{-1} \text{ Na}_2\text{HPO}_4/\text{KH}_2\text{PO}_4$ solution) to

eliminate peroxyxynitrite decay under acidic conditions. The DCFH-DA assay was added within 5 min after sample withdrawal.

Changes of *pH* and electrolytic conductivity in plasma treated water were measured by *pH* and conductivity probes (WTW, *Adwa*).

2.5. Solutions

Four different aqueous solutions of different buffering activities and electrical conductivities σ (0.6 and $6 \text{ mS} \cdot \text{cm}^{-1}$) were used for plasma treatment experiments. The solutions were prepared by the addition of phosphates and/or NaCl salt into deionized water ($\sigma = 1 \mu\text{S} \cdot \text{cm}^{-1}$, *pH* = 5.5). The chemical and physical properties of these solutions designated in this paper as water, saline, PB, and PBS are listed in Table 1. The initial temperature of all solutions was ambient ($\approx 20^\circ\text{C}$). NaH_2PO_4 solutions designated as water were used to mimic the natural conductivity of tap water ($\approx 0.6 \text{ mS} \cdot \text{cm}^{-1}$) that was largely used in our previous bio-decontamination experiments^[20,21] and because NaH_2PO_4 has similar chemical composition with the phosphate buffer (PB), but no buffering activity. PB solutions were prepared from Na_2HPO_4 and KH_2PO_4 salts at the ionic strength (concentration) sufficiently controlling the *pH* value of plasma treated solutions close to physiological *pH* value and providing nearly the same initial conductivities as in water ($0.6 \text{ mS} \cdot \text{cm}^{-1}$) or saline ($6 \text{ mS} \cdot \text{cm}^{-1}$).

3. Results and Discussion

3.1. Transient Spark Discharge

Electrical parameters and emission spectra of the transient spark discharge (TS) operating in atmospheric air were documented in detail in our previous works.^[28,29] The typical voltage and current waveforms of positive TS discharge in 10 mm gap used in this work (with electro-spray of water) are shown in Figure 3.

When a positive HV of a few kV was applied to the point electrode, streamer corona appeared, typical with small

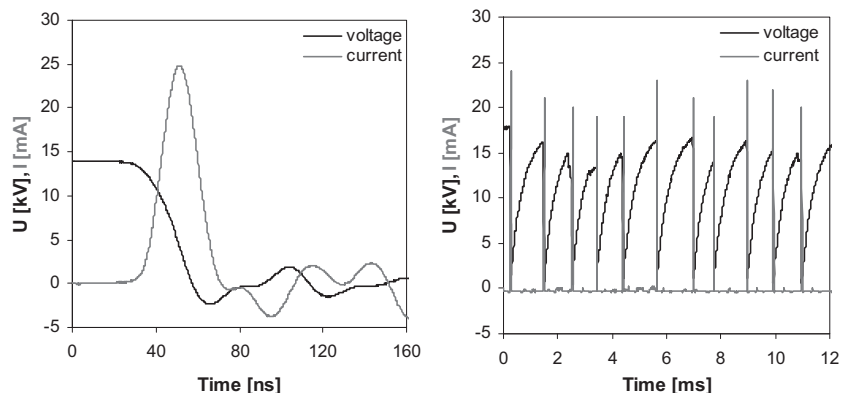


Figure 3. Typical voltage and current waveforms of TS discharge with electro-spray of water in (a) ns time scale – one pulse, and (b) ms time scale – several pulses.

current pulses of streamers ($\approx 10 \text{ mA}$) with a repetitive frequency of 10–30 kHz, during which the discharge voltage remained fairly constant. As the positive voltage was further increased (to $\approx 12 \text{ kV}$ in 10 mm gap), the streamers established a conductive channel that gradually heated, thus enhancing the reduced electric field E/N , which eventually led to a spark breakdown with excessive current pulse. In our case, the spark pulse current was limited by a ballast resistor R ($10 \text{ M}\Omega$) that dropped the voltage as the current increased, and by a small capacity C between the electrodes (order of 10 pF). C is a sum of the internal capacity of the discharge gap and the capacities of the HV cable and the voltage probe. Thus, when the sparks forms, it is only transient since the energy discharged from C is small (0.1–1 mJ per pulse). After the pulse, C was recharged by a growing potential on the stressed electrode and triggered a new pulse. This transient spark became then a repetitive streamer-to-spark transition discharge, with each spark pulse ($\approx 1 \text{ A}$) preceded by one or a sequence of streamer pulses. The repetitive frequency of pulses was 0.5–10 kHz, and increased with the applied voltage. Due to the very short pulse duration (≈ 10 – 100 ns) given by the small C and a limiting R , the plasma could not reach equilibrium conditions and remained at relatively low gas temperature

Table 1. Aqueous solutions used for plasma electro-spray treatment experiments. Initial and final values of solution conductivity σ and *pH* are denoted as “*i*” and “*f*”, respectively.

Name	Composition of solution	σ_i [$\text{mS} \cdot \text{cm}^{-1}$]	<i>pH</i> _{<i>i</i>}	σ_f [$\text{mS} \cdot \text{cm}^{-1}$]	<i>pH</i> _{<i>f</i>}
Water	$7.5 \text{ mmol} \cdot \text{L}^{-1} \text{ NaH}_2\text{PO}_4$	0.60	5.5	1.04	3.3
PB	$2 \text{ mmol} \cdot \text{L}^{-1} \text{ Na}_2\text{HPO}_4/\text{KH}_2\text{PO}_4$ buffer	0.60	6.9	0.70	6.2
Saline	$72 \text{ mmol} \cdot \text{L}^{-1} \text{ NaCl}$	6.35	6.7	6.85	2.8
PBS	$72 \text{ mmol} \cdot \text{L}^{-1} \text{ NaCl} + 2 \text{ mmol} \cdot \text{L}^{-1} \text{ Na}_2\text{HPO}_4/\text{KH}_2\text{PO}_4$ buffer	5.95	6.9	6.40	6.2

Final values indicate the state directly after spraying the solution through the plasma.

(≈ 500 – $1\,500$ K), depending on frequency, i.e., dissipated power.

With water electro-spray through TS, a great care was taken to keep the constant electrical parameters throughout each experiment since the water spray substantially perturbed the discharge regularity (especially the pulse frequency jittered). In addition, the radius of curvature of the needle deteriorated in time, which influenced the streamer formation and subsequent streamer-to-spark transition that is essential in this discharge mechanism. In order to keep the constant power dissipated into the discharge, the pulse frequency was controlled at ≈ 1 kHz. The typical applied power used in this work was 1–2 W, with energy 1–2 mJ per pulse.

3.2. Bactericidal Effect of Plasma Water Treatment

Bacterial suspensions of *E. coli* (CCM3954) were dispersed in aqueous solutions and electro-sprayed through the transient spark discharge. Figure 4 shows the bactericidal efficacy of the discharge expressed as logarithmic reduction of *E. coli* population obtained in four different aqueous solutions (Table 1), directly after plasma treatment and 5 h later. The results here and in the following figures are presented as medians with error bars showing 25 and 75 percentiles. Up to 7-log reduction in *E. coli* population was obtained both in water and in saline solutions. In buffered solutions (PB and PBS), significantly lower bactericidal effect was obtained (about 1-log reduction). Almost no change of the bactericidal effect was observed when bacteria were left in the plasma treated water or saline for 5 h longer. On the other hand, the decontamination effect increased substantially 5 h after plasma

treatment in PB and PBS but without further pH change. This indicates the ongoing post-discharge biochemical processes in the plasma treated solutions that were also reported previously.^[3,4,14,18] The results obtained in water and PB also indicate that the bactericidal effect was not affected by a lower value of the initial solution conductivity ($0.6\text{ mS}\cdot\text{cm}^{-1}$), i.e., by lower ionic strength of these solutions, since comparable bactericidal effects were obtained in saline and PBS ($6\text{ mS}\cdot\text{cm}^{-1}$). Thus, the ionic strength of water and PB was sufficient to rule out bacteria destruction caused by osmotic stress in these solutions. On the other hand, the lower ionic strengths of water and PB solutions make them more suitable for chemical analysis of the effects caused by plasma treatment (e.g., using ion chromatography). This is why we used these diluted solutions in parallel with saline solutions for this study of plasma induced effects on bacteria.

Apparently, the bactericidal effect of plasma treated solutions was accompanied with the significant changes in pH. In water and saline solutions, the pH value decreased down to $\text{pH} \approx 3$ along with the increase of the solution conductivity (Table 1). Experiments with the buffered solutions (PB and PBS) proved their sufficient buffer capacity, i.e., their pH value remained fairly constant upon treatment by the discharge ($\text{pH} 6.9$) or decreased very little (Table 1). As opposed to $\text{pH} \approx 3$ reached in water and saline after plasma treatment, $\text{pH} \approx 6.2$ in dilute PB can be still considered non-acidic. As a consequence of non-acidic environment, the bactericidal effect was strongly reduced in PB and PBS compared to non-buffered solutions. However, additional tests (not shown) performed to evaluate whether low pH is the main bactericidal agent showed that the nitric or hydrochloric acid solution of the same pH did not lead to the same bactericidal effects. In agreement with^[2,13,14,18] we confirm that rather acidic environment in synergy with plasma agents leads to the bacterial inactivation. These effects were investigated in more detail and are reported in the following sections.

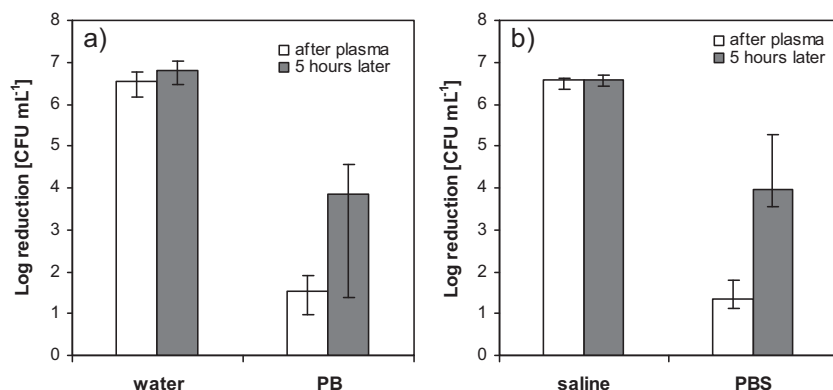


Figure 4. *E. coli* log reduction directly after plasma treatment and 5 h later obtained in different aqueous solutions in dependence on the initial solution conductivity σ_0 and pH: (a) water ($\sigma_i = 0.6\text{ mS cm}^{-1}$, $\text{pH} \approx 3.3$ after plasma) and PB solutions ($\sigma_i = 0.6\text{ mS cm}^{-1}$, $\text{pH} \approx 6.2$ after plasma); (b) saline solution ($\sigma_i = 6.35\text{ mS cm}^{-1}$, $\text{pH} \approx 2.8$ after plasma) and PBS ($\sigma_i = 5.95\text{ mS cm}^{-1}$, $\text{pH} \approx 6.2$ after plasma). The results here and in the following figures are presented as medians with error bars showing 25 and 75 percentiles.

of the same pH did not lead to the same bactericidal effects. In agreement with^[2,13,14,18] we confirm that rather acidic environment in synergy with plasma agents leads to the bacterial inactivation. These effects were investigated in more detail and are reported in the following sections.

3.3. Measurements of the Oxidative Stress

Concentrations of TBARS products indicating the cell membrane lipid peroxidation by ROS were evaluated in all tested solutions (water, PB, saline, PBS) after plasma treatment of the same samples evaluated for bactericidal effect. Figure 5 demonstrates a correlation of measured concentration of TBARS products with the bactericidal efficacy. Log reduction is

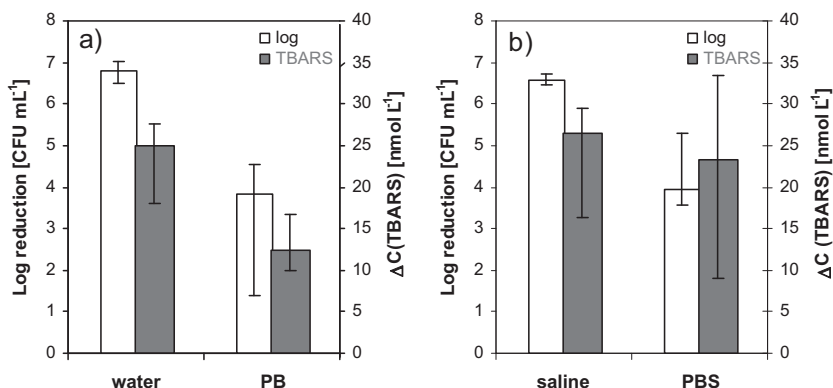


Figure 5. *E. coli* log reduction in (a) water and PB, and (b) saline and PBS, 5 h after plasma treatment, correlated with the concentrations of TBARS products $\Delta c(\text{TBARS})$ with reference concentrations subtracted.

shown after 5 h post plasma treatment because TBARS method also required at least 5 h delay post treatment. Oxidative stress is apparently lower in PB than in water, which agrees with the bactericidal effect. This correlation confirms our previous results^[20,21] and indicates that cell membrane peroxidation by ROS belongs to important mechanism in plasma bio-decontamination.

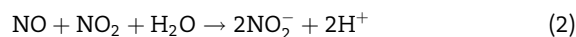
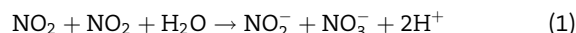
3.4. Chemical Effects Induced in Water by Plasma Treatment

In order to evaluate the mechanisms participating in bacterial inactivation, the chemical effects induced in water electro-sprayed through the transient spark were studied in more detail. Since the discharge operates in atmospheric humid air, we focused mainly on the formation of ROS and RNS. Previous measurements made by optical emission spectroscopy of TS^[29] showed a presence of atomic O, N and H, OH radicals, and the N_2^+ ions. Part of O radicals reacts with air O_2 and form ozone O_3 . There was practically no UV-C radiation detected from TS. In this work, we measured formations of hydrogen peroxide (H_2O_2), nitrites (NO_2^-), nitrates (NO_3^-), and peroxyxynitrites (ONOO^-) in plasma treated solutions. The presence of ozone in plasma treated solutions was indicated only indirectly through the occurrence of Peroxone chemistry of ozone with H_2O_2 (see later text).

3.4.1. Nitrites, Nitrates, and Hydrogen Peroxide

Figure 6 shows the concentrations of nitrites, nitrates and hydrogen peroxide obtained in water and PB solutions after spraying through the discharge. Both solutions were of the same initial conductivity ($0.6 \text{ mS} \cdot \text{cm}^{-1}$; Table 1). In water, pH decreased after the discharge from the initial value of 5.5 typically to ≈ 3.3 , while in the buffered PB solutions, pH decreased only very little (to ≈ 6.2). Figure 6

shows that non-acidic environment of PB buffers resulted in much higher concentrations of nitrites ($\approx 0.6 \text{ mmol} \cdot \text{L}^{-1}$) and slightly lower concentrations of H_2O_2 ($\approx 0.4 \text{ mmol} \cdot \text{L}^{-1}$) compared to non-buffered solutions, in which the concentrations of H_2O_2 were $\approx 0.7 \text{ mmol} \cdot \text{L}^{-1}$ and nitrites $\approx 0.2 \text{ mmol} \cdot \text{L}^{-1}$. Concentrations of nitrates were practically the same ($\approx 0.9\text{--}1 \text{ mmol} \cdot \text{L}^{-1}$). The mechanism of nitrites and nitrates formation in water is the result of dissolution of nitrogen oxides formed in air plasma by gas-phase reactions of dissociated N_2 and O_2 . Along with formation of NO_2^- and NO_3^- in the plasma treated water, dissolution of NO_x in water leads to the decrease of pH (Equation 1 and 2).^[7]



The difference in the concentrations of NO_2^- and NO_3^- measured in both plasma treated solutions (water and PB) is then a result of subsequent post-discharge reactions leading to disproportionation of nitrites into nitrates occurring under acidic conditions, which can be summarized as (Equation 3).^[7]



This route is greatly accelerated at pH below ≈ 3.5 which correlates with acid-base properties of nitrites ($\text{p}K_a = 3.3$).

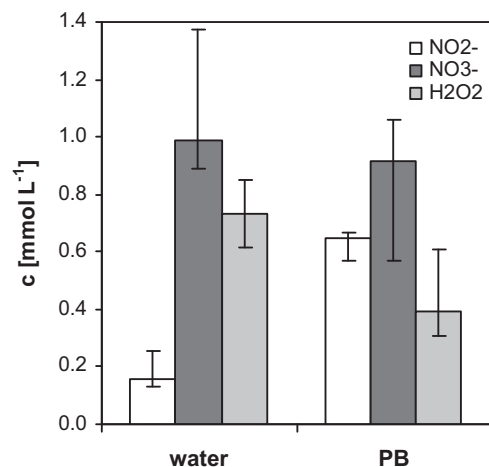
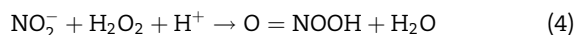


Figure 6. Nitrite (NO_2^-), nitrate (NO_3^-) and hydrogen peroxide (H_2O_2) concentrations measured in water and PB solutions after plasma treatment.

Since the only difference between buffered and non-buffered solutions was the resulting pH, it is reasonable to assume that the initial production rates of nitrites and nitrates by the discharge were the same under both conditions.

3.4.2. Peroxynitrites

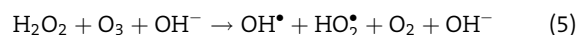
In addition, the decay of NO_2^- may also proceed via reaction with H_2O_2 (Equation 4). This route occurs under acidic conditions and proceeds via formation of peroxynitrous acid ($\text{O}=\text{NOOH}$) or its conjugate base peroxynitrite ($\text{O}=\text{NOO}^-$), which subsequently decays into the final product NO_3^- .^[30–33]



Measurement of temporal evolution of H_2O_2 concentration in plasma treated water and PB showed that H_2O_2 in water progressively decreased with time (Figure 7), which supports the involvement of H_2O_2 in the decay of NO_2^- via peroxynitrite mechanism (4). Peroxynitrites are relatively strong oxidants with a large bactericidal effect and they may significantly contribute to the inactivation process induced by air plasma in water. Under acidic conditions, their bactericidal effect is determined mainly by OH^\bullet and NO_2 radicals formed during the decomposition reaction of peroxynitrous acid.^[8] Considering the increasing acidity of the plasma treated non-buffered solutions (water, saline), it is likely that the reaction between nitrites and H_2O_2 (Equation 4) and the contribution of peroxynitrites to the plasma induced bactericidal effects might take place.

However, the results shown in Figure 6 and 7 demonstrate that the higher concentrations of H_2O_2 were determined in non-buffered solutions immediately after plasma treatment compared to buffered solutions, which is

in contradiction with the expected pH-dependent reaction between nitrites and H_2O_2 taking place in plasma treated solutions. One of the reasons for this discrepancy is ozone, which is formed by plasma in air and can dissolve into the plasma treated water and induce decomposition of H_2O_2 in buffered solutions, where reaction between H_2O_2 and ozone might take place through Peroxone process (Equation 5).^[34,35]



This process is strongly accelerated at pH above 5.5^[34] and it is the most likely the reason of lower concentrations of H_2O_2 determined in PB compared with water immediately after the plasma treatment. Thus, while changing pH of the solution, different chemistry has to be considered and direct comparison of H_2O_2 formation in solutions with different pH is not possible. However, Peroxone process can be important in PB and PBS only for relatively short time after plasma treatment due to the short lifetime of ozone in water (order of minutes). Later on, there was no further decomposition of H_2O_2 and its concentration in PB and PBS remained stable up to 5 h, in contrast to the non-buffered solutions, as demonstrated in Figure 7.

The attempt was made to measure directly the peroxynitrites formed in plasma treated solutions and to correlate their formation with the bactericidal effects obtained in plasma treated solutions in dependence on pH (water vs. PB). The example fluorescence spectra of plasma treated versus non-treated (reference) water with DCFH-DA fluorescent probe are shown in Figure 8.

It should be noted that DCFH-DA is also widely used to detect ROS in general (including H_2O_2)^[36] and our plasma treated water contained H_2O_2 that could also contribute to DCFH fluorescence. However, according to Possel et al.^[26]

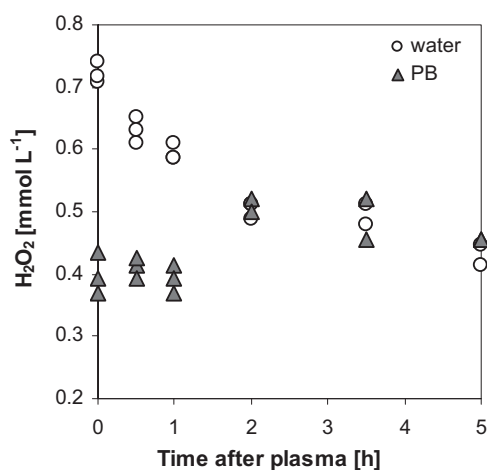


Figure 7. Temporal evolution of H_2O_2 concentration in plasma treated water and PB.

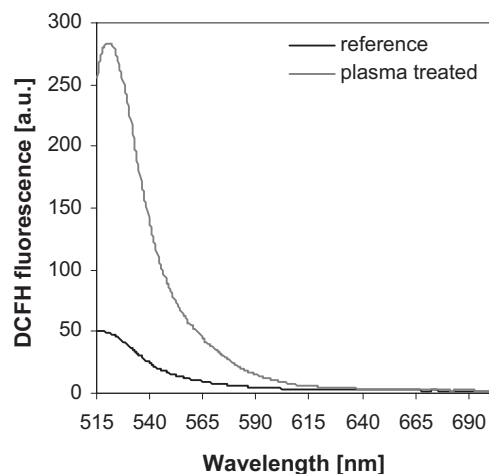


Figure 8. The example fluorescence spectra of plasma treated versus non-treated (reference) water with DCFH-DA fluorescent probe.

and Crow^[27] DCFH (as well as structurally similar fluorogenic probes such as DHR-123) displays much greater sensitivity to peroxynitrites than any other ROS including H₂O₂ or superoxide. We have experimentally confirmed this by additional tests aimed at DCFH fluorescence in H₂O₂ solutions of concentrations equivalent to H₂O₂ produced in the plasma-treated water. The fluorescence signals from 1 mmol · L⁻¹ water solution of H₂O₂, as well as 1 mmol · L⁻¹ H₂O₂ in HNO₃ solution at pH ≈ 3 (adapted to the typical pH in plasma treated water) were considerably lower than from the plasma-treated water (without the presence of bacteria), as demonstrated in Figure 9. Since the DCFH fluorescence in plasma-treated water was much stronger than that would simply result from H₂O₂, we attributed this fluorescence to peroxynitrites. Peroxynitrites are highly reactive under acidic conditions, their lifetime is very short, therefore their analysis in plasma treated solutions was so far possible only qualitative with concentrations estimated in the order of tens of μmol · L⁻¹. Higher ONOO⁻ concentrations in plasma treated water are supposedly expected immediately after plasma exposure.

Nevertheless, Figure 10 shows that the relative amounts of peroxynitrites ONOO⁻ measured by fluorescence spectroscopy in plasma treated solutions correlate directly with the bactericidal efficacy, similarly to oxidation stress measured by TBARS (Figure 5). These qualitative measurements indicate an important role of

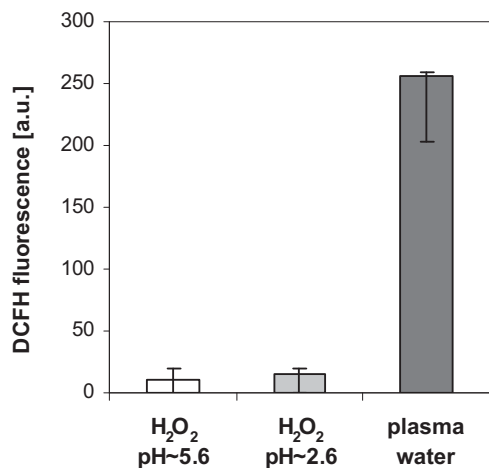


Figure 9. The fluorescence signals from: 1 mmol · L⁻¹ water solution of H₂O₂ at pH ≈ 5.6; 1 mmol · L⁻¹ H₂O₂ in HNO₃ solution at pH ≈ 2.6 (adapted to the typical pH in plasma treated water); and plasma-treated water.

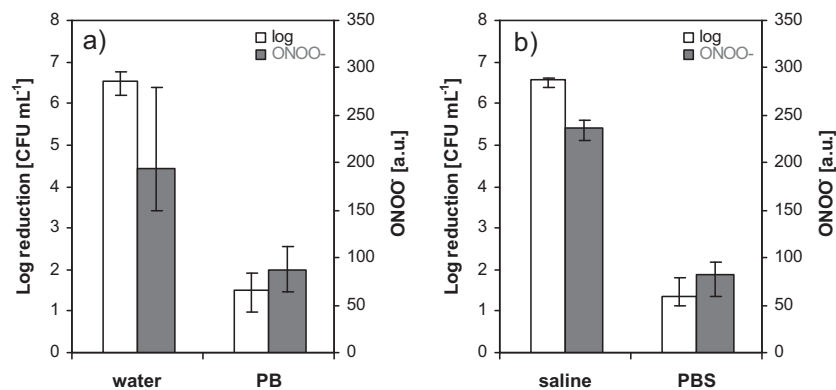
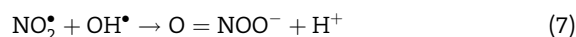


Figure 10. *E. coli* log reduction in (a) water and PB solutions, and (b) saline and PBS, directly after plasma treatment correlated with the relative amount of ONOO⁻ (fluorescence emission with reference subtracted).

ONOO⁻ in bio-decontamination and their possible relation to peroxidation of cell membranes, especially under acidic conditions. However, the method of ONOO⁻ absolute concentration measurement in plasma treated solutions respecting their short lifetime has to be further investigated.

Figure 6 and 10 show that the formation of ONOO⁻ does not correlate perfectly with the formations of nitrites and peroxides obtained in buffered and non-buffered solutions. We assume that the main reason for lower concentrations of nitrites determined in non-buffered solutions is their acidic disproportionation (Equation 3) rather than formation of peroxynitrous acid through the reaction of nitrites with H₂O₂ (Equation 4). It should be noted that peroxynitrites might be also formed by other pathways such as by the reaction of nitric oxide and superoxide anion radical (Equation 6) or by the reaction of NO₂ and OH[•] radicals (Equation 7).^[30–33]



However, due to the fast decay of these radicals, these two reactions might take place only directly in the plasma zone and the formation of peroxynitrite by these routes was not possible to determine by the analytical method used in this work.

3.4.3. Acidified Nitrites

At the same time, the antimicrobial properties of nitrites under acidic conditions have to be considered. Figure 11 shows the relation of NO₂⁻, NO₃⁻, and H₂O₂ concentrations with the bactericidal effect induced by plasma in water and PB. The stronger bactericidal effect in water (acidic

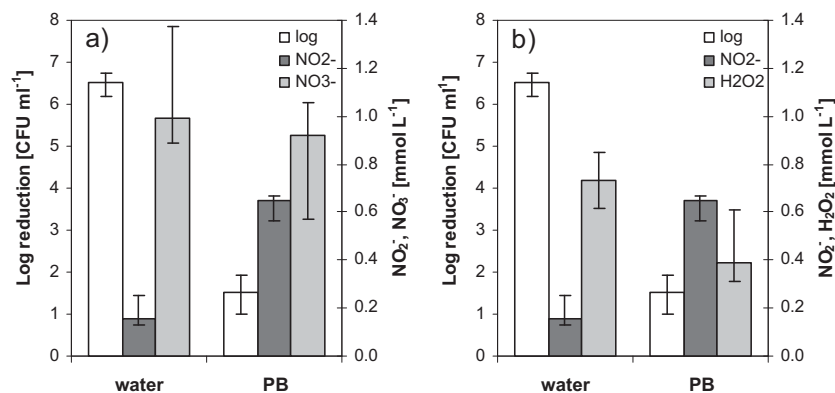
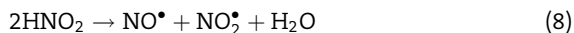


Figure 11. *E. coli* log reduction in water and PB solutions related to (a) NO₂⁻ and NO₃⁻ and (b) NO₂⁻ and H₂O₂ concentrations.

conditions) seems related with lower NO₂⁻ concentrations, as NO₂⁻ are quickly disproportionated into NO₃⁻.

Direct bactericidal effect of NO₂⁻ at acidic conditions (so-called acidified nitrites) is known and has been reported previously.^[3,19] Nitrous acid HNO₂, which is formed from nitrites under acidic conditions ($pK_a = 3.3$) is not stable and rapidly decomposes into nitrogen oxide NO[•] and nitrogen dioxide NO₂ intermediates (Equation 8) upon formation of nitrates as the final product of nitrite disproportionation (Equation 3).



The formation of cell toxic nitrogen radicals NO[•] and NO₂[•] is more likely the main reason of induced cytotoxic effect of NO₂⁻ under acidic conditions.^[14,19] In fact, it seems that acidified nitrites might be more important route of bactericidal effects caused by NO₂⁻ then through their reaction with H₂O₂ upon formation of peroxynitrites (Equation 4). Nevertheless, it is reasonable to assume that the overall bactericidal effect of the air plasma discharge involves synergistic effect of nitrites and peroxides in acidic conditions through cytotoxic activity of secondary reactive chemical species NO[•], NO₂[•], OH[•], and ONOOH.

3.4.4. Ozone and Nanoparticles

Ozone probably also contributes to the bactericidal effects under non-acidic conditions, such as at physiological pH in buffered solutions, where Peroxone chemistry between ozone and hydrogen peroxide gives additional OH[•] radicals (Equation 5) produced in post-discharge reactions in plasma treated PB and PBS. However, rather constant H₂O₂ concentration in the plasma treated PB during the time period of 5 h (Figure 7) suggests that the Peroxone processes in buffered solutions occurred just immediately after the plasma treatment and did not contribute to the subsequent enhancement of the bactericidal effect in PB and PBS 5 h

after the experiment (Figure 4). Peroxynitrite formation mechanism that requires acidic conditions (Equation 4) cannot be the reason for continuing bactericidal effects in this case as well.

A potential explanation of the observed enhancement of the bactericidal effect in the plasma treated PB and PBS after 5 h might be attributed to a possible presence of metal (iron) nanoparticles sputtered from the stainless steel needle electrode during the plasma treatment. Recently, the confluence of nanotechnology and biology has brought nanoparticles as potential antimicrobial agents. The antibacterial activity of metal nanoparticles including proposed

mechanisms against bacteria have been widely reported.^[37–42] There are evidences that metal nanoparticles can directly damage bacterial cell wall, by release of ions followed (individually or in combination) by increased membrane permeability, loss of the proton motive force and efflux of intracellular components.^[40] The antibacterial activity of the metal nanostructures depends mainly on particle size and shape, internalization, agglomeration, chemical functionalization, concentration, type of organisms etc. Silver, gold, magnesium, copper, aluminum, zinc, titanium, and iron nanoparticles have been tested for their biocidal effects.

Regarding the effect of iron nanoparticles, Mahdy et al.^[38] reported that increasing concentration of FeO substantially inhibited the growth of *E. coli*. Chatterjee et al.^[37] reported a similar effect for Fe₃O₄. Kim et al.^[39] also reported the inactivation of *E. coli* by zero-valent iron and ferrous ion nanoparticles. The main reason behind bactericidal effects of iron nanoparticles is the oxidative stress possessed by ROS generated by metal oxides.^[43] Nanoparticles may penetrate into bacteria cell membranes and, e.g., react with intracellular oxygen to create hydrogen peroxide, which consequently reacts with ferrous ions via the Fenton reaction and produces OH radicals. Iron nanoparticles can produce various ROS, including superoxide (O₂^{-•}), OH and singlet oxygen (¹O₂). The ROS production has been found in diverse metal oxide nanoparticles that besides oxidative stress may result in inflammation and consequent damage to proteins and DNA in bacteria and eventually cause disruption of the cell membrane.^[37]

In our experiments, it is possible that metal (iron) nanoparticles sputtered from the stainless steel needle electrode during the discharge operation may contaminate the plasma treated solutions and can play a role in bacteria inhibition. The electrode erosion process cannot be avoided, however, we could not prove these nanoparticles experimentally (iron ions were not detected in our plasma

treated solutions by the applied analytical methods). We might only speculate that the magnitude of the erosion was probably small since the discharge treatment time was short (~5 min) and the applied power was low (1–2 W). In water and saline, where the bactericidal effect was very strong (6–7 logs), the possible effect of nanoparticles to bacteria (although possibly present) was completely overwhelmed by other chemical effects. In PB and PBS, where immediate bactericidal effect was only 1–2 logs, the contribution of nanoparticles might be more dominant and could explain the progress of the bactericidal effect in longer post-discharge treatment times (5 h). However, extensive further work with analytical techniques designed for nanoparticles and detailed investigations of their contribution to the plasma chemistry and bactericidal effects have to be performed to confirm this hypothesis.

4. Conclusion

We investigated chemical and bactericidal effects induced in water or saline non-buffered and buffered solutions contaminated with *E. coli* bacteria by electro-spraying through the cold air plasma of transient spark. The plasma treatment led to the acidification and the production of nitrites, nitrates, peroxides, and peroxy-nitrites in the liquid. At lowered pH, nitrites were quickly oxidized to nitrates and this was associated with the strong bactericidal effect. At neutral pH in buffered solutions, nitrites were less oxidized and the bactericidal effect was weaker. The bactericidal effects correlated with the relative amount of the formed peroxy-nitrites, as well as with the oxidative stress induced in cell membranes measured by TBARS method. The estimated concentrations of peroxy-nitrites were, however, too low compared to the measured nitrites and H₂O₂ to claim their reaction as the main mechanism of peroxy-nitrite formation and to consider peroxy-nitrites as the key bactericidal agent. Instead, rather the synergistic effects of nitrites and peroxides in acidic conditions seem the most responsible for bactericidal properties of water electro-sprayed through air plasma. Ozone and iron nanoparticles sputtered from the electrodes can also contribute to the bactericidal effect.

Acknowledgements: This work was supported by Slovak Grant Agency VEGA 1/0668/11, Slovak Research and Development Agency APVV SK-CZ-0179-09, the Grant Agency of AS CR (No. IAAX00430802), the Czech Science Foundation (No. 104/09/H080), and the Ministry of Education, Youth and Sports of the Czech Republic (No. MEB0810116).

Received: August 17, 2012; Revised: February 27, 2013; Accepted: March 8, 2013; DOI: 10.1002/ppap.201200113

Keywords: bacteria; cold plasma; peroxides; peroxy-nitrites; nitrites; water electro-spray

- [1] M. Laroussi, *IEEE Trans. Plasma Sci.* **2002**, *30*, 1409.
- [2] S. Ikawa, K. Kitano, S. Hamaguchi, *Plasma Process. Polym.* **2010**, *7*, 33.
- [3] M. J. Traylor, M. J. Pavlovich, S. Karim, P. Hait, Y. Sakiyama, D. S. Clark, D. B. Graves, *J. Phys. D: Appl. Phys.* **2011**, *44*, 472001.
- [4] M. Naitali, G. Kamgang-Youbi, J. M. Herry, M. N. Bellon-Fontaine, J. L. Brisset, *Appl. Environ. Microbiol.* **2010**, *76*, 7662.
- [5] D. Dobrynin, G. Friedman, A. Fridman, A. Starikovskiy, *New. J. Phys.* **2011**, *13*, 103033.
- [6] Y. Akishev, N. Trushkin, M. Grushin, A. Petryakov, V. Karal'nik, E. Kobzev, V. Kholodenko, V. Chugunov, G. Kireev, Y. Rakitsky, I. Irkhina, "Inactivation of microorganisms in model biofilms by an atmospheric pressure pulsed non-thermal plasma," in *Plasma for Bio-Decontamination, Medicine and Food Security, NATO Science for Peace and Security Series A: Chemistry and Biology*, Z. Machala, K. Hensel, Y. Akishev, Eds., Springer, Dordrecht, Netherlands **2012**, Ch. 12, p. 149.
- [7] P. Lukes, B. R. Locke, J. L. Brisset, "Aqueous-phase chemistry of electrical discharge plasma in water and in gas-liquid environments," in *Plasma Chemistry and Catalysis in Gases and Liquids*, V. I. Parvulescu, M. Magureanu, P. Lukes, Eds., Wiley-VCH, Weinheim, Germany **2012**, Ch. 7, p. 241.
- [8] P. Lukes, J. L. Brisset, B. R. Locke, "Biological effects of electrical discharge plasma in water and in gas-liquid environments," in *Plasma Chemistry and Catalysis in Gases and Liquids*, V. I. Parvulescu, M. Magureanu, P. Lukes, Eds., Wiley-VCH, Weinheim, Germany **2012**, Ch. 8, p. 309.
- [9] S. G. Joshi, M. Cooper, A. Yost, M. Paff, U. K. Ercan, G. Fridman, G. Friedman, A. Fridman, A. D. Brooks, *Antimicrob. Agents Chemother.* **2011**, *55*, 1053.
- [10] V. N. Vasilets, A. B. Shekhter, "Nitric oxide plasma sources for bio-decontamination and plasma therapy," in *Plasma for Bio-Decontamination, Medicine and Food Security, NATO Science for Peace and Security Series A: Chemistry and Biology*, Z. Machala, K. Hensel, Y. Akishev, Eds., Springer, Dordrecht, Netherlands **2012**, Ch. 30, p. 393.
- [11] S. P. Kuo, O. Tarasenko, J. Chang, S. Popovic, C. Y. Chen, H. W. Fan, A. Scott, M. Lahiani, P. Alusta, J. D. Drake, M. Nikolic, *New. J. Phys.* **2009**, *11*, 115016.
- [12] D. Dobrynin, K. Arjunan, A. Fridman, G. Friedman, A. M. Clyne, *J. Phys. D: Appl. Phys.* **2011**, *44*, 034021.
- [13] K. Oehmigen, M. Hahnel, R. Brandenburg, C. Wilke, K. D. Weltmann, T. von Woedtke, *Plasma Process. Polym.* **2010**, *7*, 250.
- [14] K. Oehmigen, J. Winter, M. Hahnel, C. Wilke, R. Brandenburg, K. D. Weltmann, T. von Woedtke, *Plasma Process. Polym.* **2011**, *8*, 904.
- [15] J. L. Brisset, B. Benstaali, D. Moussa, J. Fanmoe, E. Njoyim-Tamungang, *Plasma Sources Sci. Technol.* **2011**, *20*, 034021.
- [16] J. L. Brisset, D. Moussa, A. Doubla, E. Hnatiuc, B. Hnatiuc, G. K. Youbi, J. M. Herry, M. Naitali, M. N. Bellon-Fontaine, *Ind. Eng. Chem. Res.* **2008**, *47*, 5761.
- [17] Y. Z. Tang, X. P. Lu, M. Laroussi, F. C. Dobbs, *Plasma Process. Polym.* **2008**, *5*, 552.
- [18] J. Julák, V. Scholtz, S. Kotúčová, O. Janoušková, *Phys. Med.* **2012**, *28*, 230239.

- [19] D. B. Graves, *J. Phys. D: Appl. Phys.* **2012**, *45*, 263001.
- [20] Z. Machala, I. Jedlovsky, L. Chladekova, B. Pongrac, D. Giertl, M. Janda, L. Sikurova, P. Polcic, *Eur. Phys. J. D* **2009**, *54*, 195.
- [21] Z. Machala, L. Chladekova, M. Pelach, *J. Phys. D: Appl. Phys.* **2010**, *43*, 222001.
- [22] B. Pongrac, Z. Machala, *IEEE Trans. Plasma Sci.* **2011**, *39*, 2664.
- [23] G. M. Eisenberg, *Ind. Eng. Chem. Anal. Ed.* **1943**, *15*, 327.
- [24] C. N. Satterfield, A. H. Bonnell, *Anal. Chem.* **1955**, *27*, 1174.
- [25] G. Alsterberg, *Biochem. Z.* **1925**, *159*, 36.
- [26] H. Possel, H. Noack, W. Augustin, G. Keilhoff, G. Wolf, *FEBS Lett.* **1997**, *416*, 175.
- [27] J. P. Crow, *Nitric Oxide: Biol. Chem.* **1997**, *1*, 145.
- [28] M. Janda, V. Martisovits, Z. Machala, *Plasma Sources Sci. Technol.* **2011**, *20*, 035015.
- [29] Z. Machala, M. Janda, K. Hensel, I. Jedlovsky, L. Lestinska, V. Foltin, V. Martisovits, M. Morvova, *J. Mol. Spec.* **2007**, *243*, 194.
- [30] J. S. Beckman, T. W. Beckman, J. Chen, P. A. Marshall, B. A. Freeman, *Proc. Natl. Acad. Sci. USA* **1990**, *87*, 1620.
- [31] J. S. Beckman, W. H. Koppenol, *Am. J. Physiol. Cell Physiol.* **1996**, *271*, C1424.
- [32] S. Goldstein, G. L. Squadrito, W. A. Pryor, G. Czapski, *Free Radic. Biol. Med.* **1996**, *21*, 965.
- [33] G. L. Squadrito, W. A. Pryor, *Free Radic. Biol. Med.* **1998**, *25*, 392.
- [34] J. Staehelin, J. Hoigne, *Environ. Sci. Technol.* **1982**, *16*, 676.
- [35] G. Merenyi, J. Lind, S. Naumov, C. V. Sonntag, *Environ. Sci. Technol.* **2010**, *44*, 3505.
- [36] C. P. Lebel, H. Ischiropoulos, S. C. Bondy, *Chem. Res. Toxicol.* **1992**, *5*, 227.
- [37] S. Chatterjee, A. Bandyopadhyay, K. Sarkar, *J. Nanobiotechnol.* **2011**, *9*, 34.
- [38] S. A. Mahdy, Q. J. Raheed, P. T. Kalaichelvan, *Int. J. Modern Eng. Res.* **2012**, *2*, 578.
- [39] J. Y. Kim, H.-J. Park, C. Lee, K. L. Nelson, D. L. Sedlak, J. Yoon, *Appl. Environ. Microbiol.* **2010**, *76*, 7668.
- [40] J. Díaz-Visurraga, C. Gutiérrez, C. von Plessing, A. García, "Metal nanostructures as antibacterial agents," in *Science Against Microbial Pathogens: Communicating Current Research and Technological Advances, Microbiology Series No 3*, vol. 1, A. Méndez-Vilas, Ed., Formatex, Badajoz, Spain **2011**, p. 210.
- [41] E. Casals, E. Gonzalez, V. F. Puentes, *J. Phys. D: Appl. Phys.* **2012**, *45*, 443001.
- [42] R. V. Ravishankar, B. A. Jamuna, "Nanoparticles and their potential application as antimicrobials," in *Science Against Microbial Pathogens: Communicating Current Research and Technological Advances, Microbiology Series No 3*, vol. 1, A. Méndez-Vilas, Ed., Formatex, Badajoz, Spain **2011**, p. 197.
- [43] H. Sies, *Exp. Physiol.* **1997**, *82*, 291.